NASA
Technical
Paper
2266

January 1984

Dynamic Behavior of Spiral-Groove and Rayleigh-Step Self-Acting Face Seals

Eliseo DiRusso

NASA

ERRATA

NASA Technical Paper 2266

DYNAMIC BEHAVIOR OF SPIRAL-GROOVE AND RAYLEIGH-STEP SELF-ACTING FACE SEALS

Eliseo DiRusso
January 1984

Page 9, figure 9: The abscissa scale should be 0, 2.5, 5.0, 7.5, 10.0×10^{-3}.

Page 12, figure 16: The plots shown apply to an outward-pumping spiral-groove seal and should appear in figure 19.

Page 14, figure 19: The plots shown apply to an inward-pumping spiral-groove seal and should appear in figure 16.

NASA Technical Paper 2266

1984

Dynamic Behavior of Spiral-Groove and Rayleigh-Step Self-Acting Face Seals

Eliseo DiRusso

Lewis Research Center
Cleveland, Ohio

NASA
National Aeronautics
and Space Administration

Scientific and Technical Information Office

1984

Summary

Tests were performed to determine the dynamic characteristics of five self-acting face seal configurations: (1) Rayleigh-step lift-pad (2) inward-pumping spiral-groove, grooves on primary ring (3) inward-pumping spiral-groove, grooves on seal seat (4) outward-pumping spiral-groove, 36 grooves (5) outward-pumping spiral-groove, 18 grooves. The outside diameter of all the seals was 9.4 cm (3.70 in.). The tests were performed with ambient air at room temperature and atmospheric pressure. The pressure drop across the seal faces was zero, and the seal face load was a constant 73 N (16.4 lb). The tangential velocity at the outside diameter of the seals ranged from 34.5 m/sec (113 ft/sec) at 7000 rpm to 83.7 m/sec (274 ft/sec) at 17 000 rpm. The primary parameters measured in the tests were film thickness, seal seat axial motion, and seal frictional torque. These data were recorded as functions of time by a transient recorder, digitized and permanently stored on minicomputer floppy disks. The minicomputer was used to plot the data as functions of time.

A significant finding was that both of the inward-pumping seals exhibited two distinct film thickness vibratory modes which were dependent on speed: a low-amplitude mode, with a frequency of twice shaft speed, occurred at all speeds below approximately 11 000 rpm; and a high-amplitude mode, with a frequency of four times shaft speed, occurred at all speeds above approximately 11 000 rpm. The transition from one mode to the other was instantaneous (i.e., as the speed was slowly increased, the film thickness vibratory mode snapped from the low to high-amplitude mode). There was no seal face contact for either of the two modes. The placement of the spiral-grooves (i.e., on the primary ring versus on the seal seat) had no effect on the dynamic behavior of the seals or on the average film thicknesses, which were identical for each case.

The average measured film thicknesses were in excellent agreement with theoretical predictions for the low-amplitude vibration mode, but were much higher than theoretical predictions for the high-amplitude mode. This confirms that seal vibrations tend to produce higher film thicknesses than theoretical predictions which are based on steady state conditions.

Two distinct levels of seal frictional torque were observed for this seal. The torque level for the low-amplitude mode was considerably less than that for the high-amplitude mode.

The Rayleigh-step and both outward-pumping seals did not exhibit the high-amplitude film thickness vibration mode at any speed. Their dynamic responses were, in general, similar to the dynamic response of the inward-pumping seals for the low-amplitude mode.

The number of grooves (36 or 18) on the outward-pumping seals had no significant effect on film-thickness dynamic response. The average film thickness was comparable, at least at the higher speeds. The 18-groove configuration, however, had a minimum speed for self-acting operation of 12 500 rpm and the 36-groove configuration, 10 000 rpm. A potential instability may exist for the outward-pumping spiral-groove seals (at least for these tests) when they are operated near their minimum speed for self-acting operation.

Introduction

A self-acting face seal is one which employs hydrodynamic bearing technology to create a thin air film between the seal faces. This film enables the seal to operate in a noncontacting mode and, in doing so, greatly extends the life of the seal. Since this type of seal operates without face contact, it can be operated at much higher sliding speeds than contacting types using the same seal materials. Two popular types of film generating mechanisms (located on one of the seal faces) are either the Rayleigh-step lift-pad or spiral-grooves. These are discussed in detail in reference 1. Both types produce a thin film, generally of the order of 0.0051 mm (0.0002 in.). The film is generated as a result of the relative motion between the seal faces. This motion causes the sealed fluid to be pumped between the faces, resulting in a pressure rise which separates the faces. Reference 2 discusses the application of the computer program SEALSG (ref. 3) to calculate steady-state film thickness for a spiral-groove seal application in counter-rotating shafts.

Self-acting seals, however, are prone to instability or vibration of the primary ring (ref. 4). This behavior has been known for years but continues to be a problem area. During recently completed tests at the Lewis Research Center (ref. 1) in which the objective was to measure the steady-state film thickness for various self-acting geometries, peculiar vibratory modes for the film thickness were observed. Also, considerable differences occurred between measured and theoretical film predictions. Seal vibration was suspected as the major contributor to these differences.

A second series of tests was performed using the same test rig used in the tests of reference 1, but with enhanced data recording and processing capabilities. Because the rig was not designed specifically for performing dynamic tests, the tests were limited to determining the amplitude response of the film thickness as a function of time in response to the inherent vibratory motion of the seal seat (i.e., programmed seal seat motions could not be induced). However, it was felt that considerable insight

into the dynamic behavior of self-acting seals could be gained by using this rig to test various seal configurations under identical conditions. Another compromise was that secondary seal friction, a very important parameter affecting face seal vibration, could not be varied.

The objectives of the tests were to

(1) Gain insight into the dynamic behavior of self-acting seals

(2) Characterize the vibration patterns for self-acting seals

(3) Establish experimental baseline data for future comparison to theoretical dynamic models for self-acting seals.

Apparatus

Seal Test Apparatus

The seal test rig (fig. 1) consisted of a vertically mounted shaft supported radially by two tilting-pad air journal bearings, 28 cm (11 in) apart. The test seal mounted at the lower end of the shaft served as a thrust bearing for the shaft. An air turbine powered by shop air (fig. 1) mounted at the top of the rig assembly was used to drive the shaft. Compressed shop air was used to float the tilting-pad air journal bearings.

The test seal assembly (figs. 2 and 3) consisted of four basic parts: (1) seal seat, (2) primary ring (carbon face seal), (3) secondary seal (segmented carbon ring seal), and (4) carrier. The seal seat was fastened to the shaft by a central nut and rotated with the shaft. The primary ring was retained by the carrier, which fastened to the self-alining gimbal support (fig. 3). The secondary seal (fig. 3) was a segmented, circumferential seal made of carbon graphite which mated with a chrome plated surface on an Invar carrier. A gimbal support permitted the primary ring to aline itself with the seal seat. The gimbal support was mounted on a radial air journal bearing and an air thrust bearing (fig. 3). These bearings were pressurized with compressed shop air. Further details of the basic rig are given in references 5 to 7.

Seal pressurization (for startup and shutdown only) was provided by compressed shop air ducted through a passage in the seal housing (fig. 3). This was used to prevent the rubbing of the seal faces during startup and coastdown when the shaft speed was too low to maintain separation of the seal faces. The air pressure required to raise the seal seat clear of the primary ring was 15.2 kPa (2.2 psig). A pressure transducer was used to monitor the air pressure. The compressed shop air used to drive the turbine, to pressurize the the tilting-pad air journal bearings, and to provide pneumostatic seal pressurization

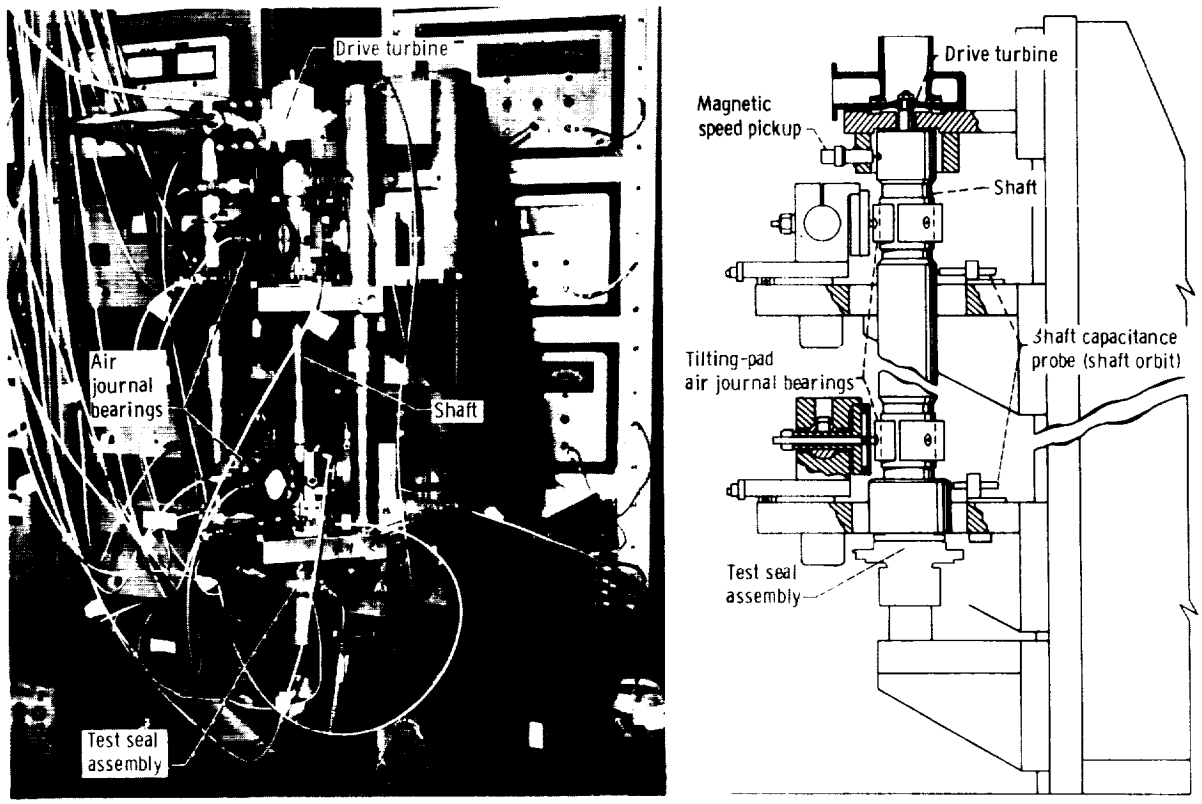

Figure 1. – Seal test apparatus.

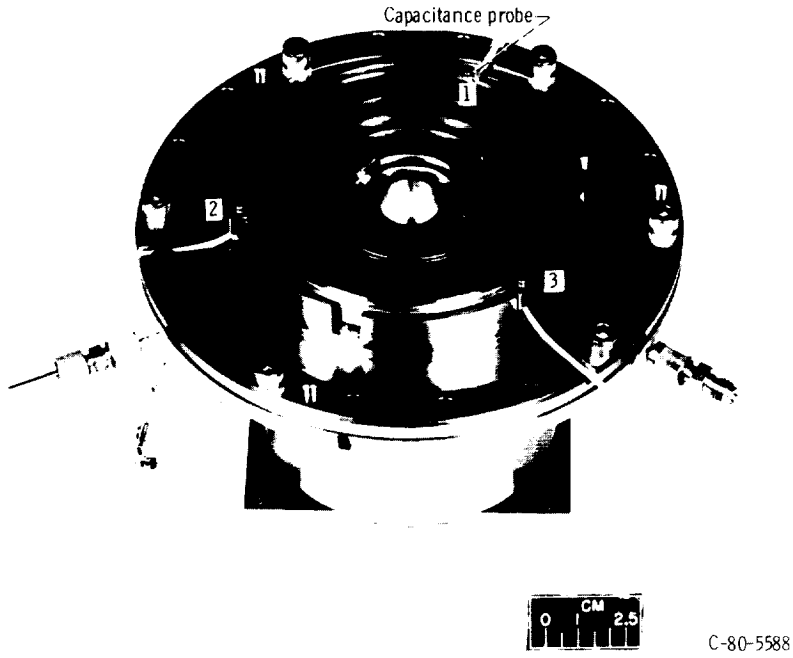

Figure 2. – Seal assembly (Rayleigh-step lift-pad seal shown).

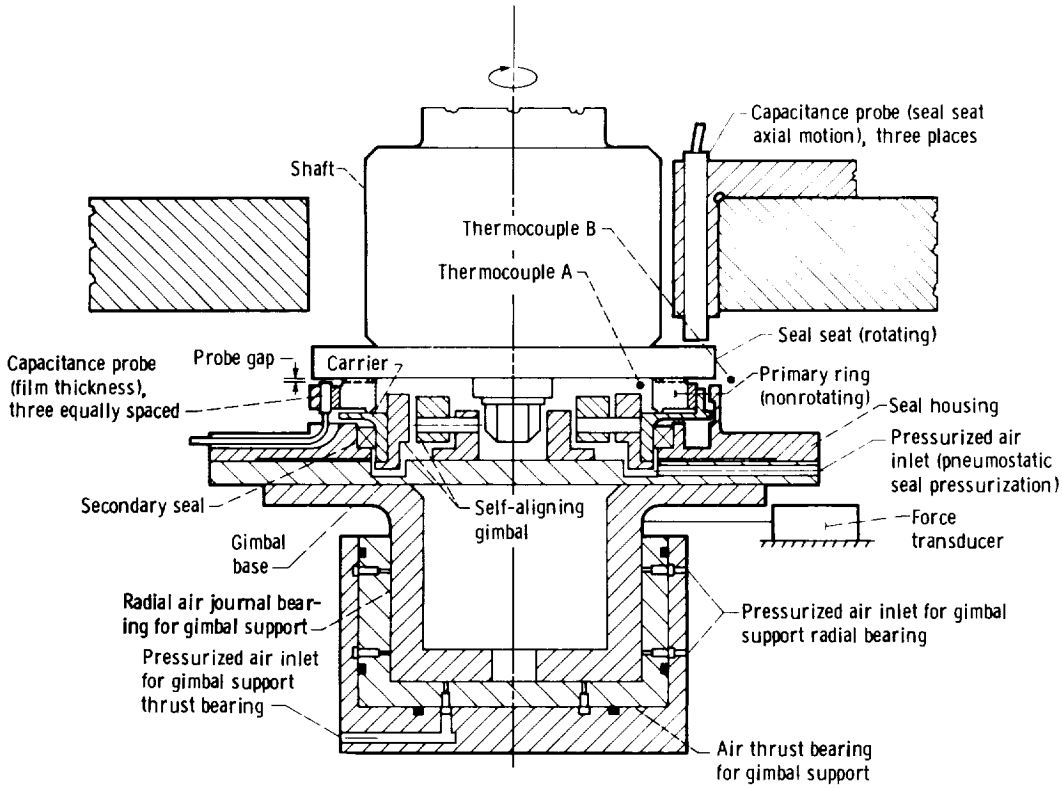

Figure 3. – Schematic of seal assembly and self-alining gimbal support.

was filtered (10 μm) to remove moisture, oil vapor, and solid particles.

Test Seal Configurations

The five self-acting face seal configurations tested were (1) Rayleigh-step lift-pad; (2) inward-pumping spiral-groove, grooves on primary ring; (3) inward-pumping spiral-groove, grooves on seal seat; (4) outward-pumping spiral-groove, 36 grooves; and (5) outward-pumping spiral-groove, 18 grooves.

The Rayleigh-step, lift-pad, self-acting geometry is shown in figure 4. Note that the self-acting geometry was machined on the surface of the carbon primary ring. Table I gives dimensions for the Rayleigh-step lift-pads. Reference 1 contains further details of this seal assembly. The seal seat for this configuration was simply a flat disk.

The inward-pumping spiral-groove, grooves on seal seat, is shown in figure 5(a). Figure 5(b) shows details of the primary ring for this seal. The spiral-groove geometry for the inward-pumping, grooves on primary ring, seal were identical to those shown in figures 5(a) and (b) except that the grooves were on the primary ring and the seal seat was simply a flat disk. Table II gives dimensions for the inward-pumping spiral-groove seals. The inward-pumping seals were optimized (i.e., lift force was maximized for this geometry). The computer program of reference 3 was used to optimize the lift force. The parameters that were varied to achieve the optimization were (1) spiral groove angle, (2) groove to land width ratio, (3) groove depth, and (4) number of grooves.

Figure 6(a) shows the self-acting geometry of the outward-pumping 36-spiral-groove seal and seal seat. The 18-groove configuration is identical to this except for the number of grooves. It should be noted that changing the number of grooves while maintaining the same groove width essentially changes the groove to land width ratio. Therefore, the 36-groove configuration has a groove to land width ratio of 1.63, in contrast to 0.45 for the 18-groove configuration. Table III gives dimensions for the outward-pumping spiral-groove seals. Figure 6(b) shows details of the primary ring. Note that the self-acting geometry was machined on the seal seat and the primary ring was a flat surface.

The material for all of the seal seats (rotating face) tested was Monel 502. The material for all of the primary rings tested was carbon graphite.

Instrumentation

The film thickness between the seal seat and the primary ring was directly measured by three capacitance probes mounted as shown in figures 2 and 3. These probes were equally spaced around the circumference and located at a radius of 5.23 cm (2.06 in.) as shown in figure 7. The initial gap between the probes and the seal seat was 0.076 mm (0.003 in.) when the seal seat was contacting the primary ring. The linear measuring range of these probes was 0 to 0.25 mm (0 to 0.010 in.). These three probes were cemented into the primary ring retainer (figs. 2 and 3) and individually calibrated in a calibration

TABLE I. - RAYLEIGH-STEP LIFT-PAD SEAL DIMENSIONS

Seal outside radius cm (in.)	4.699 (1.850)
Annular groove outside radius cm (in.)	4.084 (1.608)
Pad length, cm (in.)	1.826 (0.719)
Pad width, cm (in.)	0.516 (0.203)
Pad depth, cm (in.)	0.0018 (0.0007)
Land length, cm (in.)	0.932 (0.367)

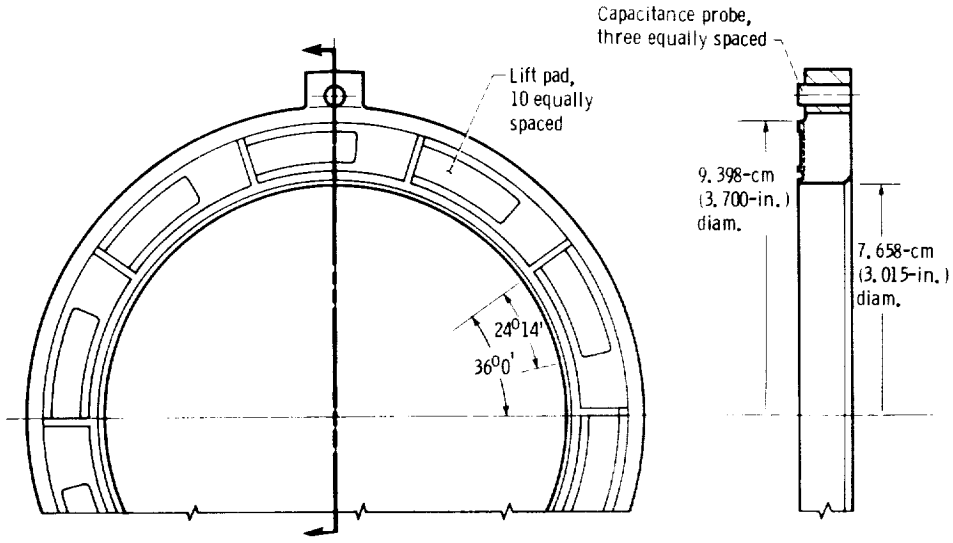

Figure 4. - Details of Rayleigh-step lift-pad primary ring.

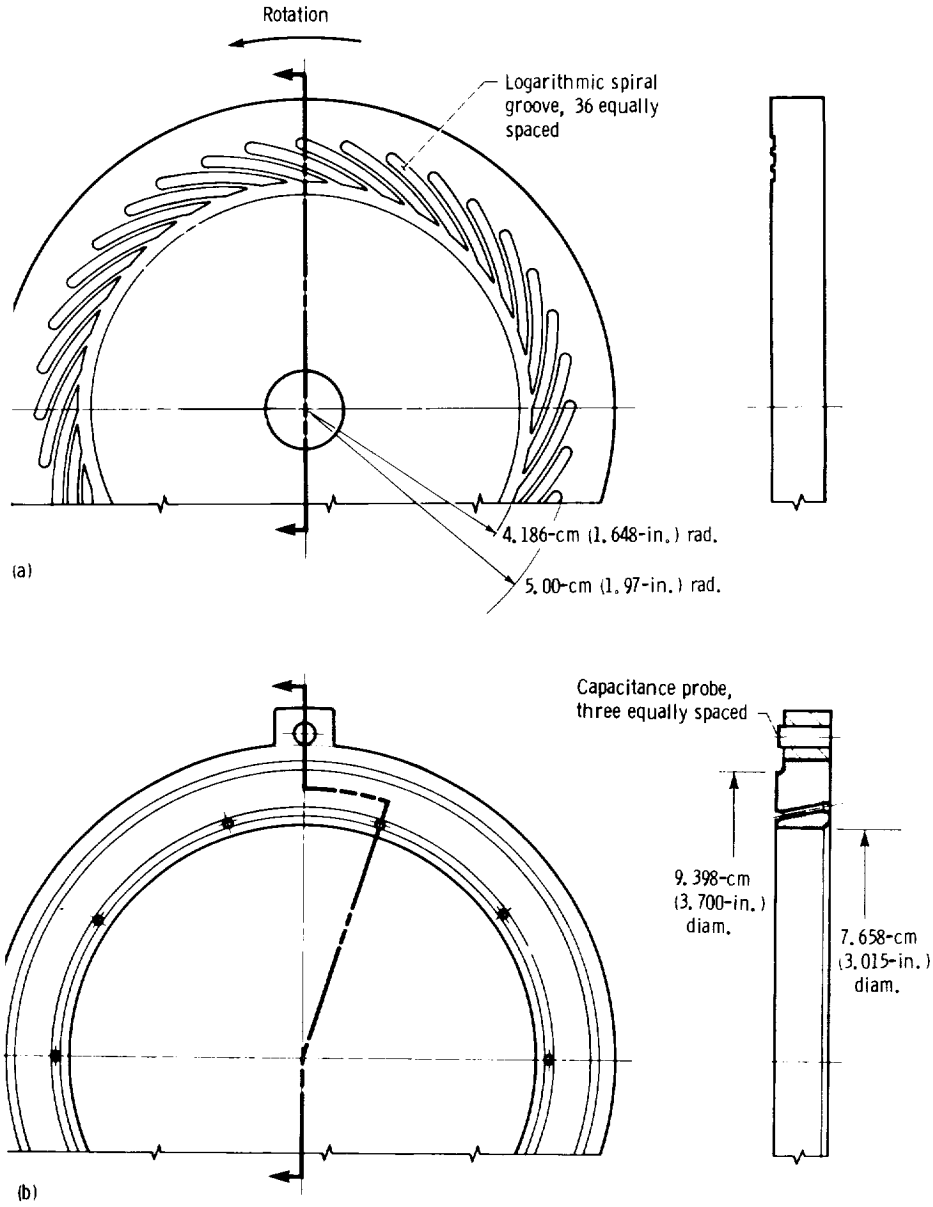

(a) Seat.
(b) Primary ring.

Figure 5. – Details of inward-pumping spiral-groove seals. (Grooves shown on seal seat).

TABLE II. – INWARD-PUMPING SPIRAL-GROOVE SEAL DIMENSIONS

Outside radius, cm (in.)	4.699 (1.850)
Inside radius, cm (in.)	4.084 (1.608)
Seal band radius, cm (in.)	4.186 (1.648)
Spiral-groove depth, cm (in.)	0.0015 (0.0006)
Groove width (measured circumferentially, cm (in.))	0.549 (0.216)
Land width (measured circumferentially, cm (in.))	0.229 (0.090)
Groove-to-land width ratio	2.40
Spiral groove angle, deg	20

fixture. The resolution was 0.000025 mm (0.000001 in), and the accuracy was estimated to be ±0.0005 mm (±0.00002 in.).

The seal seat axial motion was measured by three capacitance probes facing the top surface of the seal seat (fig. 3). These probes were located as shown in figure 7. The unequal circumferential spacing was due to rig space limitations. The linear measuring range of these probes was 0 to 0.25 mm (0 to 0.010 in.). Each probe was individually calibrated in a calibration fixture and installed in the rig. The resolution was 0.000025 mm

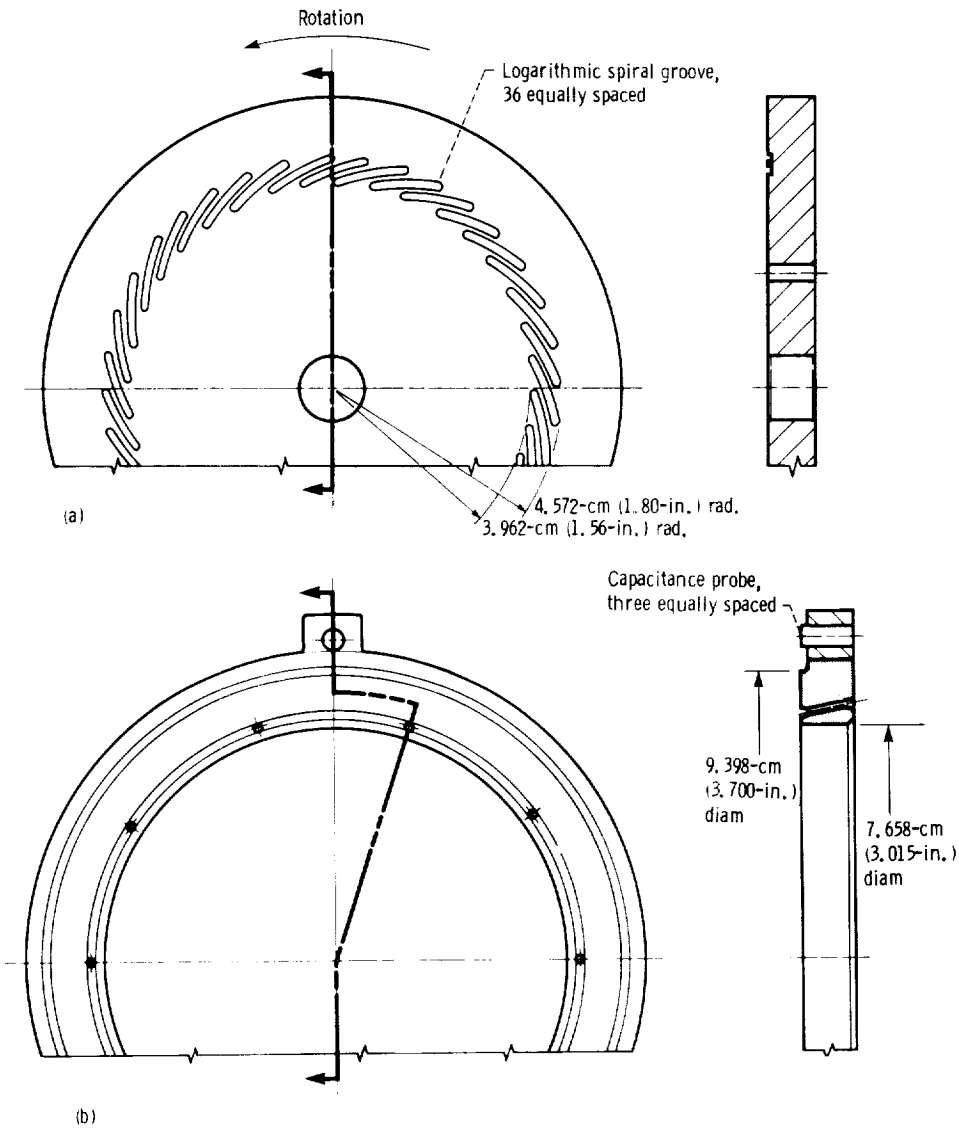

(a) Seat.
(b) Primary ring.

Figure 6. – Details of outward-pumping spiral-groove seal.

TABLE III. – OUTWARD-PUMPING SPIRAL-GROOVE SEAL DIMENSIONS

Outside radius, cm (in.)	4.699 (1.850)
Inside radius, cm (in.)	4.084 (1.608)
Seal band radius, cm (in.)	4.572 (1.800)
Spiral-groove depth, cm (in.)	0.0018 (0.0007)
Groove width (measured circumferentially, cm (in.))	0.455 (0.179)
Land width (measured circumferentially, cm (in.))	0.279 (0.110)
Groove-to-land width ratio:	
36-Groove	1.63
18-Groove	0.45
Spiral groove angle, deg	20

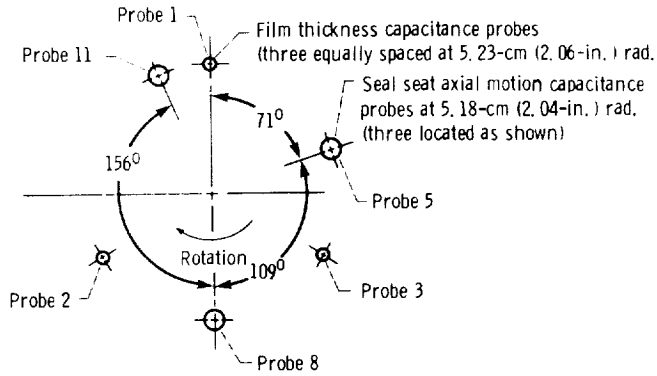

Figure 7. – Capacitance probe locations for film thickness and seal-seat axial motion. (View looking downstream.)

(0.000001 in.), and accuracy was estimated to be ±0.0005 mm (±0.00002 in.).

The shaft radial motion at each air journal bearing was monitored by two capacitance probes facing the shaft at each bearing location and mounted normal to each other. These probes are shown schematically in figure 1.

Shaft speed was sensed by a magnetic speed pickup and automatically controlled to hold any desired speed. The automatic control system varied turbine drive air pressure to maintain the desired speed.

A force transducer was mounted to the gimbal base, which was floated on air bearings (fig. 3), such that the transducer measured the tangential force between the gimbal base and ground. This mounting arrangement provided accurate and sensitive measurement of torque at the seal face. The force transducer, which was calibrated in the rig assembly by using calibrated weights, measured tangential force at a radius of 34.9 mm (1.375 in). The resolution was 0.004 N (0.001 lb), and the accuracy was estimated to be ±0.013 N (±0.003 lb).

Two thermocouples, A and B (located as in fig. 3) were used to monitor air temperature at the inside radius of the seal and outboard of the seal, respectively.

Data System

The capacitance probes which measured film thickness, seal seat axial motion, and shaft orbit were fed to capacitance probe amplifiers. The output signal from these amplifiers was proportional to the probe gaps. Frequency response of this system was −3 dB at 5 kHz. This signal was input to a transient recorder where the data were digitized at a sample rate of 20 000 samples per second and stored. This sample rate was well above the highest frequency of approximately 1500 Hz measured during the tests. The transient recorder had the capability to store up to 17 channels of data taken simultaneously (i.e., data for all input channels were recorded at the same instant in time). The signals for the seal frictional torque, speed, and seal pressure were also sent to the transient recorder and digitized. All digitized data were then sent to a minicomputer system for permanent storage on floppy disks. The dynamic data were plotted as a function of time and the average steady-state data were plotted as a function of speed using plotting routines for the minicomputer.

Signals from the film thickness probes and seal seat axial motion probes were also sent to a structural dynamics analyzer for one of the test runs to determine what frequencies were predominant during the test.

Procedure

The primary rings and seal seats were lapped flat to within three helium light bands before assembly into the test rig. The lift-pad depths and spiral-groove depths were within 0.0025 mm (0.0001 in.) of their nominal values.

The three capacitance probes that measured film thickness had an initial gap of approximately 0.076 mm (0.003 in.) when the gap at the seal faces was zero (zero film thickness). The gap for the three seal seat axial motion probes was approximately 0.178 mm (0.007 in.) when the seal faces were contacting. Amplifiers for all instrumentation were set for zero output with the seal faces firmly contacting.

Before starting the turbine drive, the seal seat was raised clear of the primary ring by activating the pneumostatic seal pressurization system. The seal pressure was set at 15.2 kPa (2.2 psig). The shaft was then rotated by hand to assure free rotation, that is, no rubbing at the seal faces. The turbine drive was then started, and the shaft was slowly accelerated to approximately 14 000 rpm. The pneumostatic seal pressure was then gradually reduced to zero gage pressure, while closely monitoring the torque and three film thickness probes. The torquemeter was used as an indicator of impending contact of the seal faces since the torque would rise rapidly in this situation. When the seal pressure was zero, the seal was self-acting and the air film between the seal faces was supporting the weight of the shaft assembly (73 N, 16.4 lb) with a positive clearance.

Once the seal was self-acting and operating stably, as indicated by the torquemeter, the shaft speed was increased to approximately 17 000 rpm (rig imposed speed limit) and allowed to stabilize. The analog data from the instrumentation were then sent to the transient recorder where they were digitized and then stored on floppy disks by the computer. The shaft speed was gradually reduced in approximately 1000-rpm increments while closely monitoring film thickness and torque. Data were recorded at each speed increment as mentioned. This process was continued until a speed was encountered at which the torque increased with further decrease in speed. At this point the speed was increased to a point where stable operation was regained.

On completion of the test, the shaft speed was set at approximately 14 000 rpm, and the pneumostatic seal pressure was set at 15.2 kPa (2.2 psig). The turbine drive air was then turned off, and the shaft was allowed to coast to a stop. The pneumostatic seal pressure was then reduced to zero. All instrumentation were recorded with the seal at rest after the seal seat was verified to be firmly resting on the primary ring. This was to assure that there were no significant zero shifts. This procedure was used for all of the seals tested.

Results and Discussion

During recently completed tests (ref. 1) at the Lewis Research Center, in which the objective was to measure

the film thickness of several spiral-groove self-acting seal configurations and a Rayleigh-step lift-pad seal, some differences in the dynamic behavior of these seals was observed. Also observed were differences in seal stability between the various configurations when operated under the same conditions. To gain more insight into the dynamics of these seals, a series of tests was conducted to document the dynamic nature of film thickness (film thickness as a function of time) in response to the inherent vibratory motions of the seal seat. For these tests, the film thickness as a function of time was the motion of the primary ring relative to the seal seat. Therefore, perfect tracking of the seal seat by the primary ring is indicated only if the film thickness is constant as a function of time (i.e., there is no periodic vibration of the film thickness).

The dynamic tests were conducted under the same conditions as the steady-state tests of reference 1. Test conditions are summarized as follows:

Seal outside diameter	9.4 cm (in.) (3.70)
Fluid medium	ambient air
Fluid temperature, °C (°F)	21 (70)
Fluid pressure, kPa (psia)	10.1 (14.7)
Pressure drop across the seal faces	0
Constant seal face load, N (lb)	73 (16.4)
Rotational speed range, rpm	7000 to 17 000 rpm
Tangential velocity, m/sec (ft/sec)	34.5 to 85.7 (113 to 274)

The tests were performed using ambient air to minimize seal distortions that could result from higher temperatures and pressures.

As previously mentioned, the data were obtained with a high-data-rate digital data recording system and the displayed on computer generated plots (see Data System). The data recorded were the film thickness at three circumferential locations and the seal seat axial motion (i.e., axial displacement of the seal seat) at three circumferential locations. The relative locations of these probes is shown in figure 7. The unequal spacing of these probes shown in the figure was due to rig space limitations. Seal frictional torque and speed were also recorded. The film thickness, seal seat axial motion, seal frictional torque, and speed were all recorded at the same instant in time for any given speed. This is important in determining the type of motion that the seal seat was experiencing (i.e., nutation or axial translation). This also permits comparison of the three film thickness probes to determine the instantaneous tilt angles for future comparison with theoretical models.

Rayleigh-Step Lift-Pad Seal

Figures 8(a) to (c) show plots of film thickness for probes 1 to 3 as functions of time for the Rayleigh-step lift-pad seal operating at 15 000 rpm. The film thickness plots are composed of a steady-state or mean component (average film thickness) and a vibratory component (a variation of film thickness as a function of time about the steady-state value). Figures 8(d) to (f) show the seal seat axial motion measured by probes 5, 8, and 11 as functions of time also for 15 000 rpm. The seal seat axial

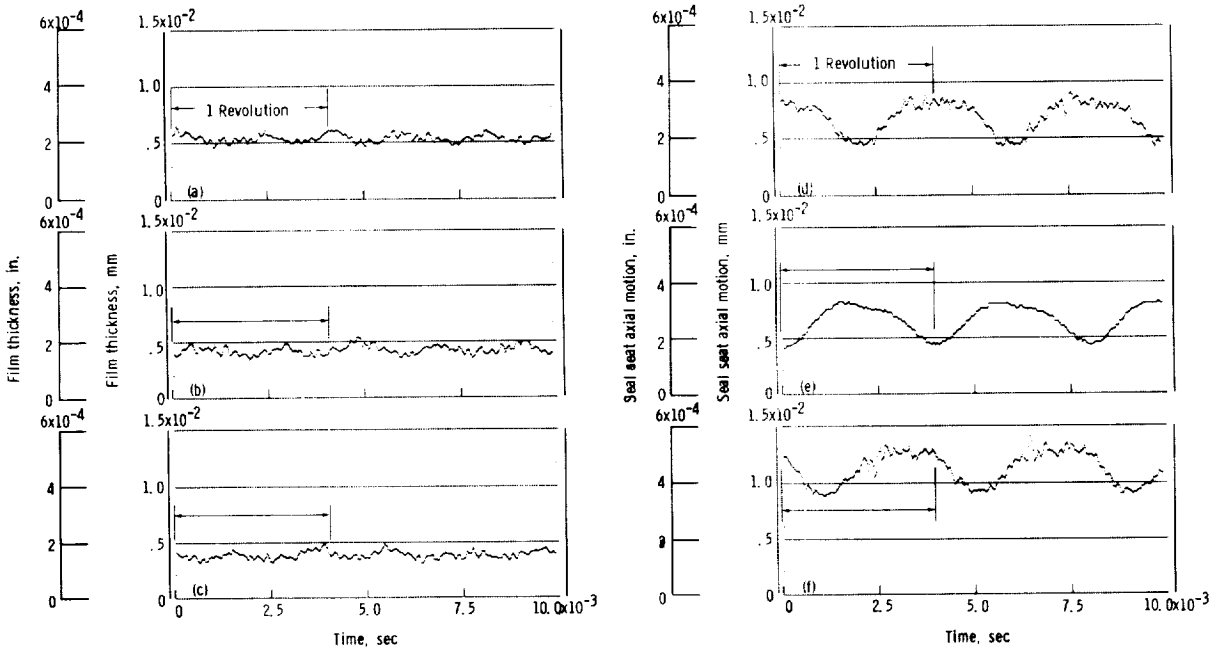

(a) Probe 1.
(b) Probe 2.
(c) Probe 3.
(d) Probe 5.
(e) Probe 8.
(f) Probe 11.

Figure 8. – Film thickness and seal seat axial motion as function of time. Rayleigh-step lift-pad seal; shaft speed, 15 000 rpm.

motion plots are also composed of a steady-state, or mean, component and a vibratory component. Observation of the three seal-seat axial motion plots indicates a complex nutating-like motion of the seal seat (deduced because the displacements were not in phase. Conversely, in-phase motion of the seal-seat axial motion probes would indicate a pure vertical translation of the seal seat.) The amplitude of the seal-seat axial motion (i.e., the vibratory component of the displacement about the mean) was 0.002 mm (0.00008 in.) and was synchronous with shaft speed. This motion was the same for the entire speed range (7600 to 17 000 rpm) and was the inherent vibratory motion of the seal seat. The film thickness plots (figs. 8(a) to (c)) show a periodic variation film thickness (about the mean) of 0.00065 mm (0.000026 in.) amplitude with a frequency of 2 cycles per shaft revolution. The film thickness plots for the entire speed range were similar to those of figures 8(a) to (c) except that the mean film thickness was higher or lower, depending on the speed.

Although the film thickness traces indicated a periodic variation with a frequency of 2 cycles per shaft revolution, the amplitude of the film thickness variation was quite small. This indicates that there was very little relative motion between the primary ring and the seal seat; hence, the primary ring was essentially tracking the seal seat. No contact occurred at the seal faces during the tests.

The plot of shaft speed as a function of time (fig. 9) indicates speed fluctuations of ±350 rpm for the time interval over which the data were taken. The seal frictional torque as a function time for 15 000 rpm (fig. 9) indicates a periodic variation of 0.14 N-cm (0.0125 in-lb) amplitude at one-half synchronous speed. Data for the speed and torque traces were taken at the same instant as the film thickness and seal seat axial motion data. They are included here to document the variation of these parameters with time during the tests.

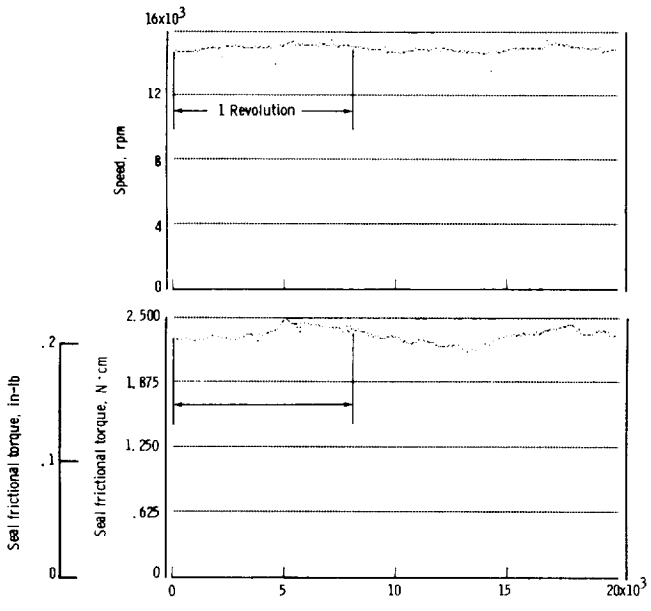

Figure 9. – Speed and seal frictional torque as fuction of time. Rayleigh-step lift-pad seal; shaft speed, 15 000 rpm.

Inward-Pumping Spiral-Groove Seal

The inward-pumping spiral-groove seal (grooves on primary ring) showed grossly different film thickness vibration patterns, depending on shaft speed. For speeds below approximately 11 000 rpm, the film thickness vibration pattern was as shown in figures 10(a) to (c) (0.0014 mm, 0.000054 in., amplitude with a frequency of 2 cycles per shaft revolution). This pattern is very similar to the Rayleigh-step lift-pad seal. For speeds above approximately 11 000 rpm the film thickness vibration pattern was as shown in figures 11(a) to (c). The film thickness traces shown in this figure are for 15 000 rpm but they are typical for all speeds above approximately 11 000 rpm. The traces indicate a high-amplitude film thickness vibration (approx 0.0075 mm, 0.0003 in.) with a frequency of approximately four times the shaft speed. Note that the minimum film thickness was very near zero. In this case the primary ring was obviously not tracking the seal seat; however, there was no evidence of face contact. This indicates the presence of a squeeze film action that precluded face contact during this vibration. It should be noted that the seal seat axial motion shown in figures 10(d) to (f) for 10 000 rpm and figures 11(d) to (f) for 15 000 rpm are essentially the same and indicate a complex nutating-like motion quite similar to that of the Rayleigh-step seal (figs. 8(d) to (f)). The seal seat axial motion experienced in the rig is therefore independent of both the type of seal and vibrational mode of the primary ring.

The interesting point here is that this seal exhibited two distinctly different modes of film thickness vibration, depending on shaft speed. The transition from the low-amplitude to high-amplitude vibration was repeated on many tests and occurred instantaneously as the speed was gradually changed. The speed at which the transition occurred was dependent on whether the speed was increasing or decreasing. Transition occured at 13 400 rpm for increasing speed and at 11 000 rpm for decreasing speed. This meant that the seal could be operated in both the low- and high-amplitude film thickness vibration modes for speeds between 11 000 and 13 000 rpm. Comparison of the average film thickness under each mode of vibration at the same speed was therefore possible. The average film thickness at 12 000 rpm for the low-amplitude mode was approximately 0.0044 mm (0.000175 in.), and for the high-amplitude mode, approximately 0.0056 mm (0.00022 in.). This shows that the high-amplitude vibration had the effect of

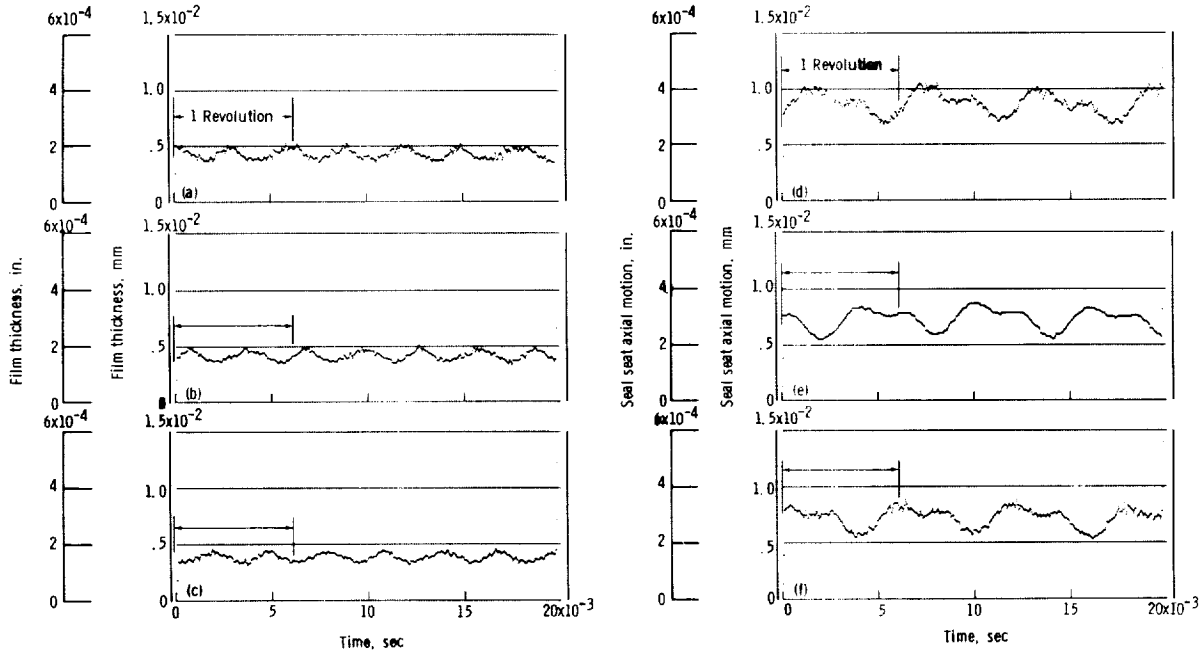

(a) Probe 1. (d) Probe 5.
(b) Probe 2. (e) Probe 8.
(c) Probe 3. (f) Probe 11.

Figure 10. – Film thickness and seal seat axial motion as function of time. Inward-pumping spiral-groove seal; grooves on primary ring; shaft speed, 10 000 rpm.

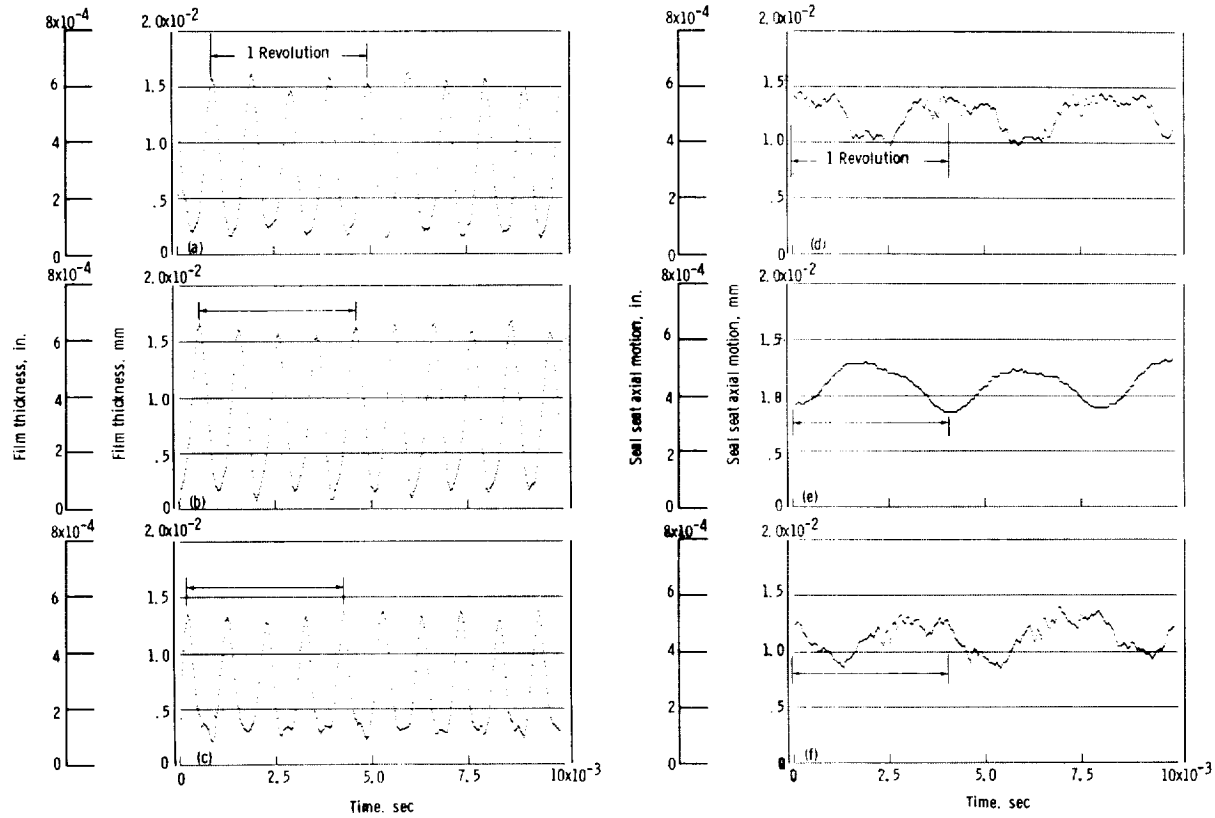

(a) Probe 1. (d) Probe 5.
(b) Probe 2. (e) Probe 8.
(c) Probe 3. (f) Probe 11.

Figure 11. – Film thickness and seal seat axial motion as function of time. Inward-pumping spiral-groove seal; grooves on primary ring; shaft speed, 15 000 rpm.

increasing the average film thickness but that the minimum film thickness, as mentioned previously, was very close to zero.

In figure 12 the experimental average film thickness as a function of speed is compared with steady-state theoretical data (ref. 1). The experimental data show excellent agreement with the theoretical data for low-amplitude vibration. However, the test data for high-amplitude vibration are much higher than the theoretical data. The curves illustrate that the primary ring vibration has a very pronounced effect on the average film thickness, particularly at higher speeds. The two film thickness vibratory modes also produced an observable effect on the seal frictional torque. The torque curves (fig. 12) show two distinct, discontinuous torque levels associated with each vibration mode; the high vibration mode producing significantly higher torque.

Figures 13 and 14 show how speed and seal frictional torque varied for the time interval over which the data were taken for the 10 000 and 15 000 rpm cases, respectively. The 10 000 rpm torque plot (fig. 13) displays a synchronous periodic oscillation of 0.18 N cm (0.016 in-lb) amplitude. Shaft speed varied ±350 rpm over the time interval.

The high-amplitude vibration with a frequency of 4 cycles per shaft revolution exhibited by this seal (figs. 11(a) to (c)) appears to indicate a stick-slip type of action. Reference 8 (p. 3-3) reports that this sort of vibration is caused by sticking of the secondary seal at the extremity of each half cycle. This causes 4 cycles per shaft revolution. Note, however, that, the same parts were used for the Rayleigh-step lift-pad seal and the inward-pumping spiral-groove (grooves on primary ring) seal except for the primary ring. The primary rings were also

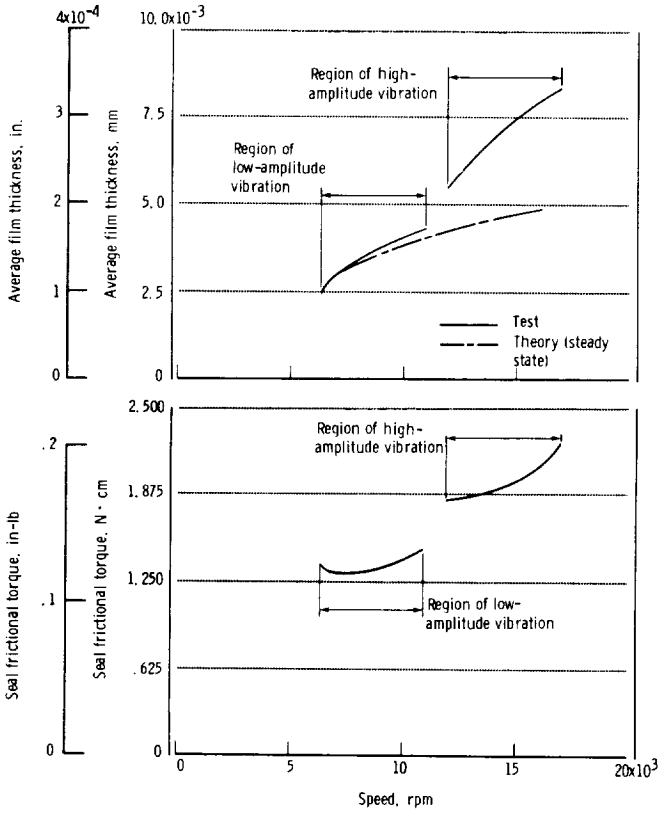

Figure 12. – Average film thickness and seal frictional torque as function of shaft speed for inward-pumping spiral-groove seal; grooves on primary ring; seal face load, 73 N (16.4 lb).

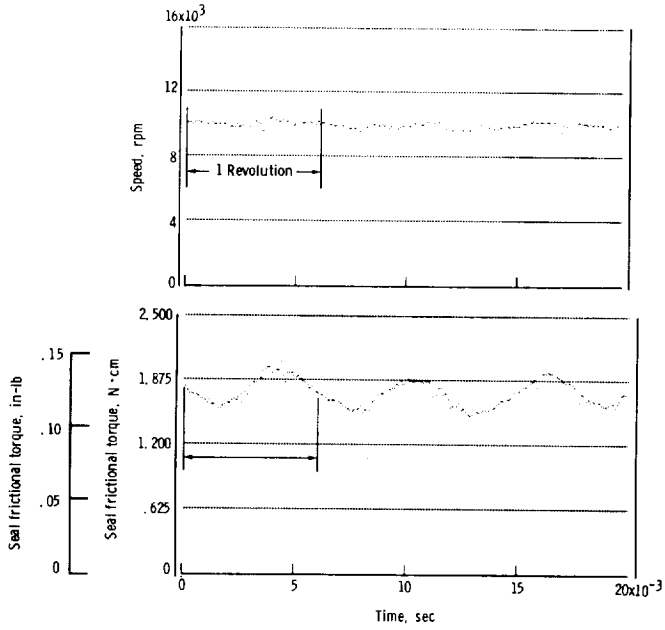

Figure 13. – Speed and seal frictional torque as function of time. Inward-pumping spiral-groove seal; grooves on primary ring; shaft speed, 10 000 rpm.

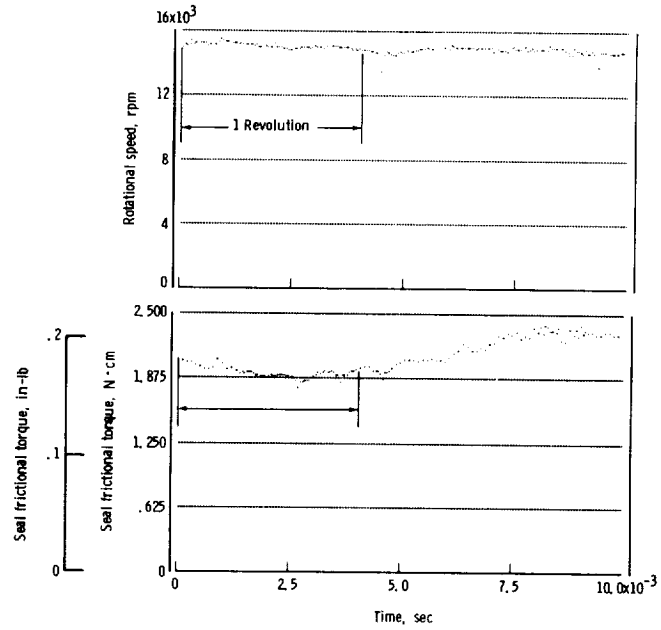

Figure 14. – Speed and seal frictional torque as function of time. Inward- pumping spiral-groove seal; grooves on primary ring; shaft speed, 15 000 rpm.

References

1. DiRusso, E.: Film Thickness Measurement For Spiral Groove and Rayleigh Step Lift Pad Self-Acting Face Seals. NASA TP-2058, Oct. 1982.
2. DiRusso, E.: Design Analysis Of A Self-Acting Spiral Groove Ring Seal For Counter-Rotating Shafts. NASA TP-2142, May 1983.
3. Mechanical Engineering Laboratory of The Franklin Research Center, A Division of The Franklin Institute: Spiral Groove Face Seal Computer Program (SEALSG). Franklin Research Center Project Number 21464, March 1979.
4. Etsion, I.: Dynamic Analysis of Noncontacting Face Seals. NASA TM-79294, May 1980.
5. Nemeth, Z. N.; and Anderson, W. J.: Dynamic Behavior Of Air-Lubricated Pivoted-Pad Journal Bearing-Rotor System. 1-Effects of Mount Stiffness and Damping. NASA TN D-5685, Feb. 1970.
6. Nemeth, Z. N.: Dynamic Behavior of Air-Lubricated Pivoted-Pad Journal-Bearing Rotor System. 2-Pivot Consideration and Pad Mass. NASA TN D-6606, Feb. 1972.
7. Nemeth, Z. N.: Operating Characteristics of a Cantilever-Mounted Resilient-Pad Gas-Lubricated Thrust Bearing. NASA TP-1438, Apr. 1979.
8. Colsher, R.; and Shapiro, W.: Steady-State and Dynamic Performance of a Gas Lubricated Seal. (F-C3452-1, Franklin Institute Research Labs; NASA Contract NAS3-16863.) NASA CR-121093, Nov. 1972.

increasing the average film thickness but that the minimum film thickness, as mentioned previously, was very close to zero.

In figure 12 the experimental average film thickness as a function of speed is compared with steady-state theoretical data (ref. 1). The experimental data show excellent agreement with the theoretical data for low-amplitude vibration. However, the test data for high-amplitude vibration are much higher than the theoretical data. The curves illustrate that the primary ring vibration has a very pronounced effect on the average film thickness, particularly at higher speeds. The two film thickness vibratory modes also produced an observable effect on the seal frictional torque. The torque curves (fig. 12) show two distinct, discontinuous torque levels associated with each vibration mode; the high vibration mode producing significantly higher torque.

Figures 13 and 14 show how speed and seal frictional torque varied for the time interval over which the data were taken for the 10 000 and 15 000 rpm cases, respectively. The 10 000 rpm torque plot (fig. 13) displays a synchronous periodic oscillation of 0.18 N cm (0.016 in-lb) amplitude. Shaft speed varied ±350 rpm over the time interval.

The high-amplitude vibration with a frequency of 4 cycles per shaft revolution exhibited by this seal (figs. 11(a) to (c)) appears to indicate a stick-slip type of action. Reference 8 (p. 3-3) reports that this sort of vibration is caused by sticking of the secondary seal at the extremity of each half cycle. This causes 4 cycles per shaft revolution. Note, however, that, the same parts were used for the Rayleigh-step lift-pad seal and the inward-pumping spiral-groove (grooves on primary ring) seal except for the primary ring. The primary rings were also

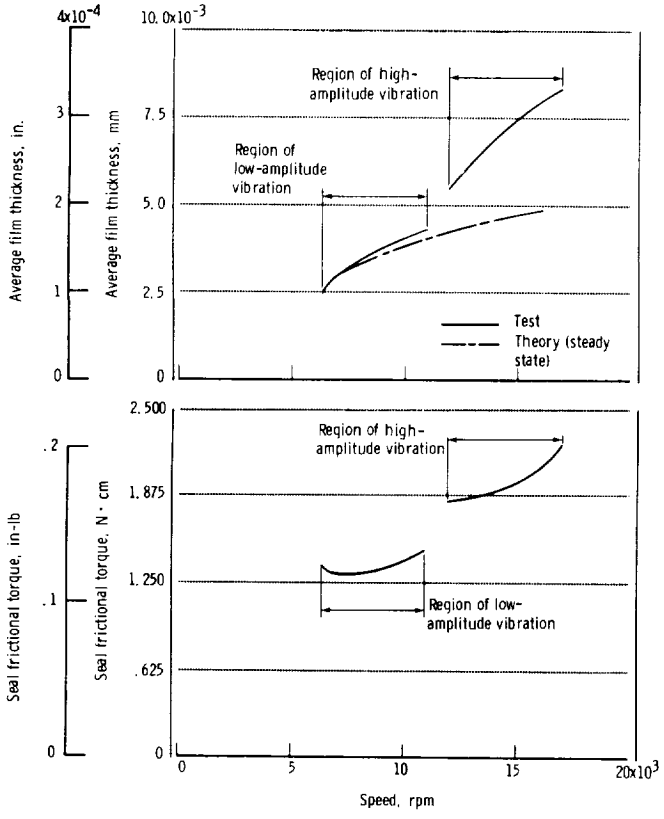

Figure 12. – Average film thickness and seal frictional torque as function of shaft speed for inward-pumping spiral-groove seal; grooves on primary ring; seal face load, 73 N (16.4 lb).

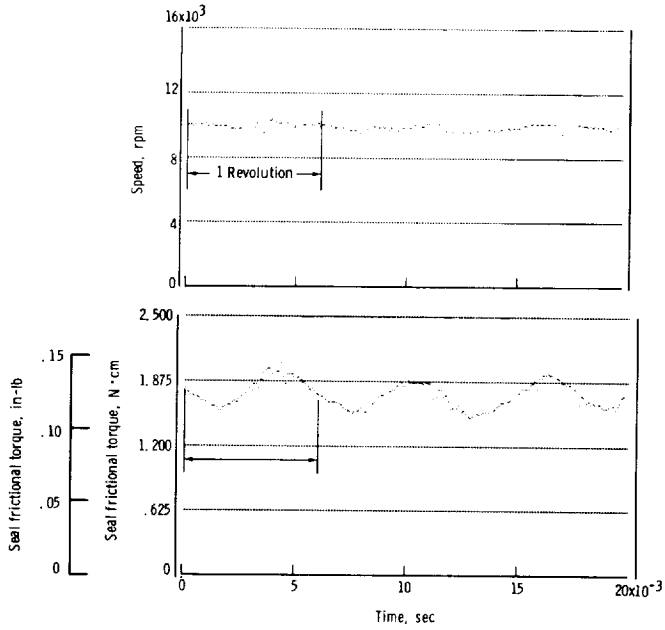

Figure 13. – Speed and seal frictional torque as function of time. Inward-pumping spiral-groove seal; grooves on primary ring; shaft speed, 10 000 rpm.

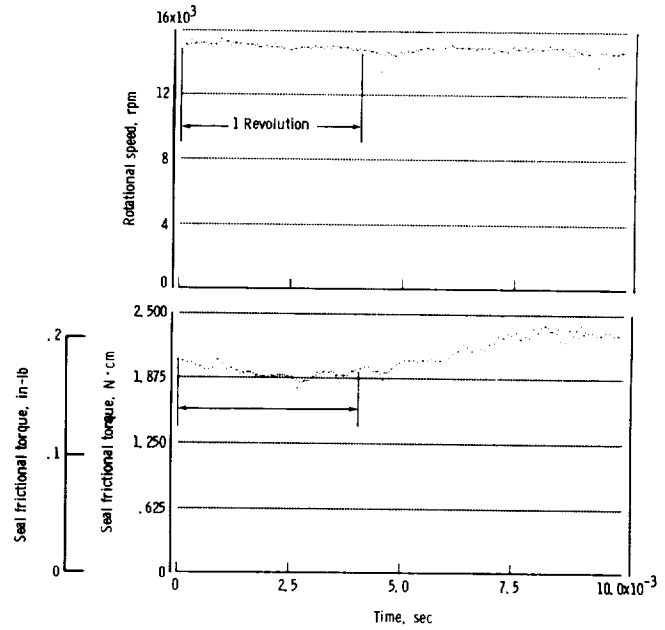

Figure 14. – Speed and seal frictional torque as function of time. Inward- pumping spiral-groove seal; grooves on primary ring; shaft speed, 15 000 rpm.

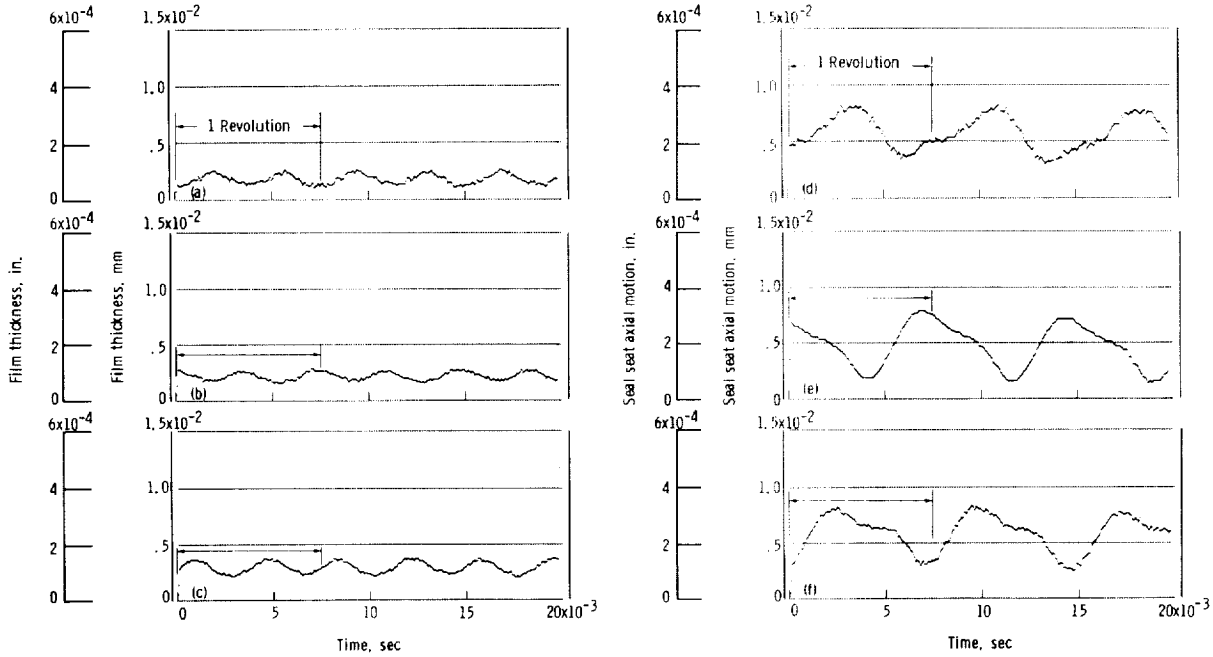

(a) Probe 1. (d) Probe 5.
(b) Probe 2. (e) Probe 8.
(c) Probe 3. (f) Probe 11.

Figure 15. – Film thickness and seal seat axial motion as function of time. Inward-pumping spiral-groove seal; grooves on seal seat; shaft speed, 8000 rpm.

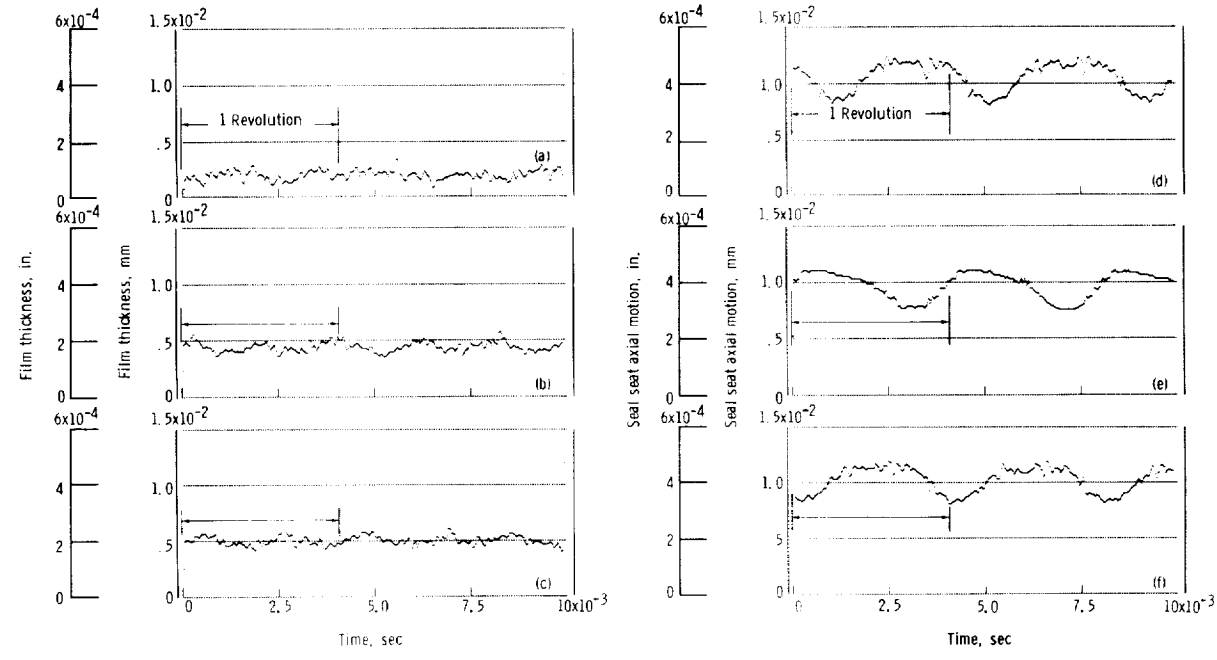

(a) Probe 1. (d) Probe 5.
(b) Probe 2. (e) Probe 8.
(c) Probe 3. (f) Probe 11.

Figure 16. – Film thickness and seal seat axial motion as function of time. Inward-pumping spiral-groove seal; grooves on seal seat; shaft speed, 15 000 rpm.

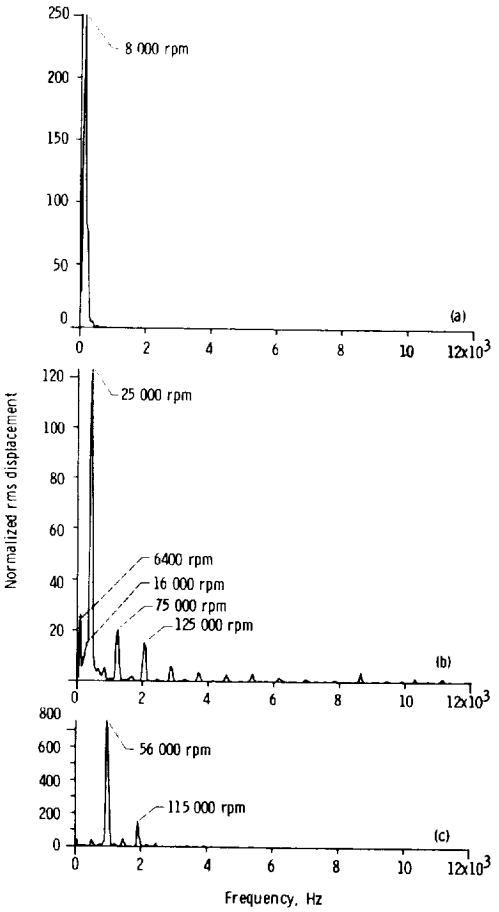

(a) Probe 8, seal seat axial motion; shaft speed, 8000 rpm.
(b) Probe 1, film thickness; shaft speed, 8000 rpm.
(c) Probe 1, film thickness; shaft speed, 15 000 rpm.

Figure 17. – Spectral analysis for inward-pumping spiral-groove seal; grooves on seal seat.

identical except for the self-acting geometry. The same secondary seal parts were used in both seals. Therefore, secondary seal friction was identical for both tests. Since the Rayleigh-step lift-pad seal did not experience the high-amplitude vibration, it would appear that this phenomenon is peculiar to the inward-pumping spiral-groove seal and not rig related.

Inward-Pumping Spiral-Groove Seal, Grooves On Seal Seat

Similar tests were performed on the inward-pumping spiral-groove seal, with grooves on seal seat, to determine the effect of placing the grooves on the seal seat (versus on the primary ring). This seal was identical to the inward-pumping spiral-groove seal (grooves on primary ring) except for groove placement. The film thickness as a function of time is shown in figures 15(a) to (c), and the seal seat axial motion is shown in figures 15(d) to (f) for 8000 rpm. Similar traces for 15 000 rpm are shown in figure 16. Clearly, the two inward-pumping seals exhibited comparable dynamic characteristics, and the placement of the spiral-grooves on the rotating or stationary ring makes no difference in behavior. The seal seat axial motion traces (figs. 15 and 16(d) to (f)) are essentially the same as for the Rayleigh-step seal (figs. 8(d) to (f)). In figures 16(a) and (b) the minimum film thickness indicated is zero. This zero is due to a slight zero shift in the instrumentation and does not indicate face contact. This was verified by inspection of the seal faces after the test.

A spectral analysis was performed during the test runs for this seal. Figure 17(a) shows that the predominant frequency for the seal seat motion was synchronous speed (8000 rpm). This is consistant with the one cycle per revolution shown in figure 15(e). Figure 17(b) shows the spectral analysis for the film thickness. A peak is indicated at 25 000 rpm, which is approximately three times the shaft speed. This peak, which must be the film thickness frequency, was expected to occur at 16 000 rpm in order to be consistent with the 2-cycles-per-revolution frequency of figure 15(a). Figure 17(c) shows the spectral analysis for film thickness at a shaft speed of 15 000 rpm. The predominant peak is at 56 000 rpm (approximately 3.7 cycles per shaft revolution), which is consistent with the film thickness frequency indicated in figure 16(a) for 15 000 rpm.

Outward-Pumping Spiral Groove Seal (36 grooves)

Figure 18 shows the film thickness variation and the seal seat axial motion as functions of time for the outward-pumping spiral-groove (36 grooves) seal at a shaft speed of 15 000 rpm. The film thickness traces for all speeds were similar to these traces (i.e., the high-amplitude film thickness vibration experienced in the inward-pumping seals was not observed in the outward-pumping seal). The film thickness traces are similar to the Rayleigh-step seal except that the the amplitude was slightly greater than that of the the Rayleigh-step seal and the film thickness frequency was synchronous with shaft speed instead of 2 cycles per shaft revolution. The seal seat axial motion shown in figures 18(d) to (f) was similar to that of the Rayleigh-step lift-pad (figs. 8(d) to (f)) and inward-pumping seals (figs. 11(d) to (f)).

This seal tended to be unstable at low speeds during the tests as discussed in reference 1. When the seal was operated near its minimum speed for self-acting operation (lift-off speed) the torque spiked instantaneously without warning. This characteristic was repeated in this series of tests; however, it occured at approximately 10 000 rpm instead of the 11 600 rpm of the previous tests. It should be noted that the inward-pumping seals and Rayleigh-step pad seal did not display this spike in the torque for any of the tests.

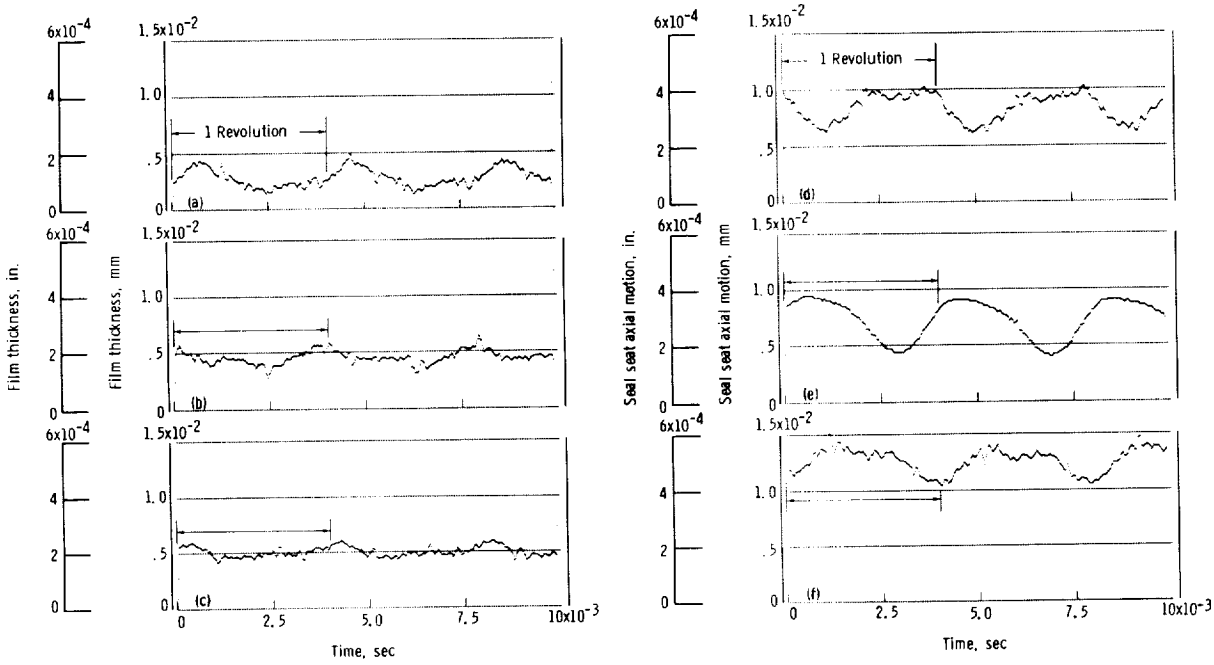

(a) Probe 1. (d) Probe 5.
(b) Probe 2. (e) Probe 8.
(c) Probe 3. (f) Probe 11.

Figure 18. – Film thickness and seal seat axial motion as function of time. Outward-pumping spiral-groove seal; 36-grooves; shaft speed, 15 000 rpm.

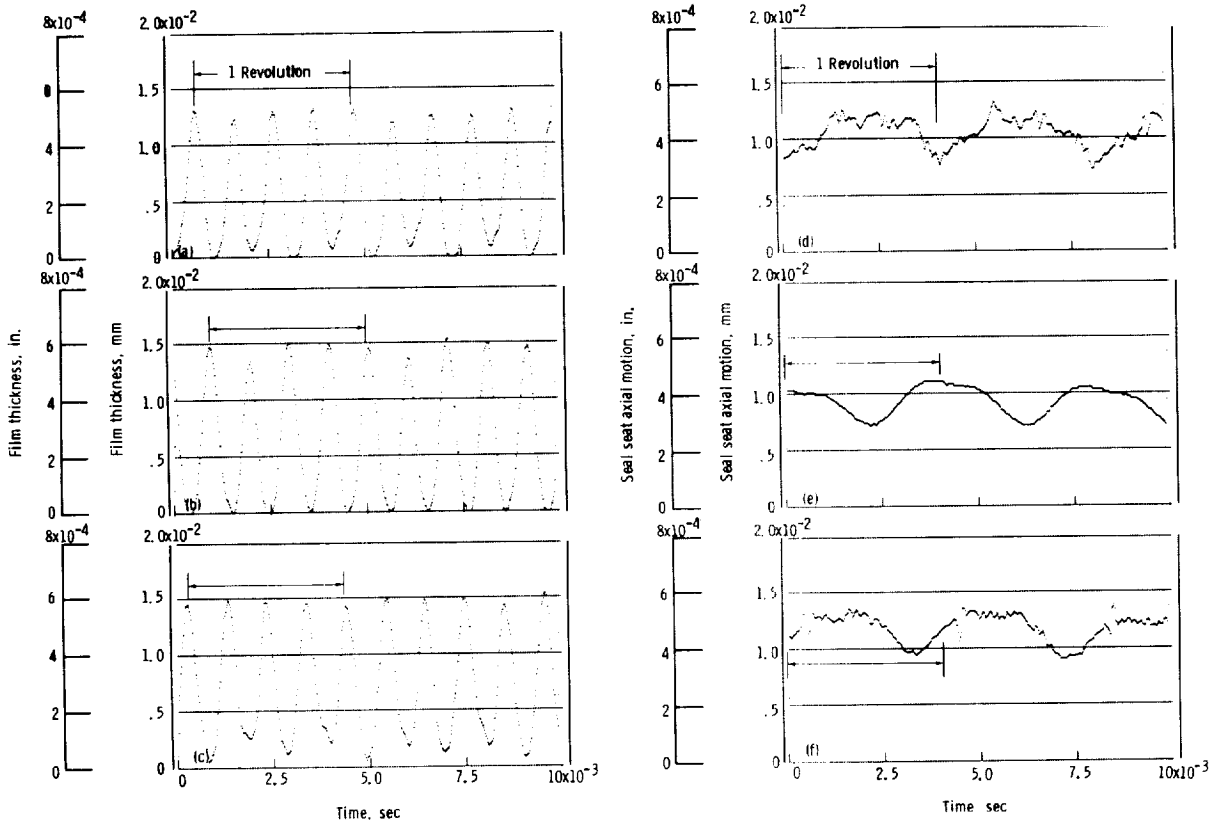

(a) Probe 1. (d) Probe 5.
(b) Probe 2. (e) Probe 8.
(c) Probe 3. (f) Probe 11.

Figure 19. – Film thickness and seal seat axial motion as function of time. Outward-pumping spiral-groove seal; 18-grooves; shaft speed, 15 000 rpm.

Outward-Pumping Spiral Groove Seal (18 grooves)

Figures 19(a) to (c) show the variation of film thickness for the outward-pumping spiral-groove seal (18 grooves) as a function of time for 15 000 rpm. This seal was identical to the 36-groove configuration except for the number of grooves and was tested to determine the effect of the number of grooves on film thickness. Comparison of these film thickness traces with those for the 36-groove seal (figs. 18(a) to (c)) indicates that the average film thickness was approximately 0.005 mm (0.0002 in.) for both cases and that the average film thickness was insensitive to the number of grooves, at least at the higher speeds. However, the minimum speed for self-acting operation for the 18-groove seal was approximately 12 500 rpm in contrast to 10 000 rpm for the 36-groove seal. This seal also exhibited the instantaneous spike in torque at its minimum speed for self-acting operation.

Dynamically, the film thickness traces were very similar to the 36-groove outward-pumping seal except that the predominant frequency was 2 cycles per shaft revolution instead of one. The film thickness traces shown for 15 000 rpm were typical for the entire speed range tested (12 500 to 17 000 rpm). This seal did not exhibit the high-amplitude 4 cycles per shaft revolution observed in the inward-pumping seals. Figures 19(d) to (f) show the seal seat axial motion for this seal. Note that these traces are the same as for all the other seals tested and were typical over the entire test speed range.

Summary of Results

Five self-acting face seal geometries were tested to gain insight into the dynamics of this type of seal and to establish baseline dynamic data for comparison with future dynamic analyses. The five seals tested were (1) Rayleigh-step lift-pad; (2) inward-pumping spiral-groove, with grooves on primary ring; (3) inward-pumping spiral-groove, with grooves on seal seat; (4) outward-pumping spiral-groove (36 grooves); and (5) outward-pumping spiral-groove (18 grooves). All of the seals had an outside diameter of 9.4 cm (3.70 in.). The seals were tested over a speed range from 7000 to 17 000 rpm for a constant face load of 73 N (16.4 lb). The tangential velocity at the outside diameter of the seals ranged from 34.5 m/sec (113 ft/sec) at 7000 rpm to 83.7 m/sec (274 ft/sec) at 17 000 rpm.

The tests revealed the following:

1. Both of the inward-pumping seals exhibited the same film thickness vibration patterns, which were dependent on shaft speed. Below approximately 11 000 rpm, a low-amplitude (0.0014 mm, 0.000054 in.) film thickness vibration pattern with a frequency of 2 cycles per shaft revolution was observed in each seal. Above approximately 11 000 rpm, the vibration pattern for both of these seals snapped into a high-amplitude (0.0075 mm, 0.0003 in.) mode with a frequency of approximately 4 cycles per shaft revolution. There was no face contact during any of the tests, even for the high-amplitude mode.

2. Both inward-pumping spiral-groove seals (grooves on primary ring or seal seat) displayed identical dynamic characteristics, indicating that the placement of the grooves on the primary ring or seal seat makes no difference. Also, the average film thickness for each of these configurations was the same.

3. Comparison of the average measured film thickness for the inward-pumping seals with the theoretical results from the computer program SEALSG (ref. 3) indicated that the high-amplitude film thickness vibration mode produced average film thicknesses much higher than the theoretical predictions. The average film thickness for the low-amplitude film thickness vibration mode showed excellent agreement with the theoretical predictions. This confirms that theoretically predicted film thickness based on steady-state conditions can be considerably too low if high seal vibration amplitudes are present in actual practice.

4. For the inward-pumping seals there were two distinct levels of seal frictional torque: One for the low-amplitude film thickness vibration mode and one for the high-amplitude mode. The two levels were discontinuous and were probably caused by the two different vibratory modes.

5. For the Rayleigh-step lift-pad seal the film thickness had a periodic variation with time of 0.00065 mm (0.000026 in.) amplitude with a frequency of 2 cycles per shaft revolution. The film thickness traces indicated that the primary ring tracked the seal seat quite well and there was no face contact during the tests.

6. The outward-pumping seals (36 and 18 grooves) displayed similar dynamic film thickness characteristics to each other and also quite similar to the Rayleigh-step seal. Average film thicknesses for the two outward-pumping seals were quite comparable; however, the 36-groove configuration had a minimum speed for self-acting operation of 10 000 rpm compared with 12 500 rpm for the 18-groove configuration.

7. When the outward-pumping seals were operated near their minimum speed for self-acting operation, the seal frictional torque tended to spike without warning, in contrast to a predictable, gradual rise in torque for the Rayleigh-step and inward-pumping seals as this speed was approached. This may indicate a possible instability (at least for these tests) for the outward-pumping seals at lift off speed.

Lewis Research Center
National Aeronautics and Space Administration
Cleveland, Ohio, August 1, 1983

References

1. DiRusso, E.: Film Thickness Measurement For Spiral Groove and Rayleigh Step Lift Pad Self-Acting Face Seals. NASA TP-2058, Oct. 1982.
2. DiRusso, E.: Design Analysis Of A Self-Acting Spiral Groove Ring Seal For Counter-Rotating Shafts. NASA TP-2142, May 1983.
3. Mechanical Engineering Laboratory of The Franklin Research Center, A Division of The Franklin Institute: Spiral Groove Face Seal Computer Program (SEALSG). Franklin Research Center Project Number 21464, March 1979.
4. Etsion, I.: Dynamic Analysis of Noncontacting Face Seals. NASA TM-79294, May 1980.
5. Nemeth, Z. N.; and Anderson, W. J.: Dynamic Behavior Of Air-Lubricated Pivoted-Pad Journal Bearing-Rotor System. 1-Effects of Mount Stiffness and Damping. NASA TN D-5685, Feb. 1970.
6. Nemeth, Z. N.: Dynamic Behavior of Air-Lubricated Pivoted-Pad Journal-Bearing Rotor System. 2-Pivot Consideration and Pad Mass. NASA TN D-6606, Feb. 1972.
7. Nemeth, Z. N.: Operating Characteristics of a Cantilever-Mounted Resilient-Pad Gas-Lubricated Thrust Bearing. NASA TP-1438, Apr. 1979.
8. Colsher, R.; and Shapiro, W.: Steady-State and Dynamic Performance of a Gas Lubricated Seal. (F-C3452-1, Franklin Institute Research Labs; NASA Contract NAS3-16863.) NASA CR-121093, Nov. 1972.

1. Report No.	2. Government Accession No.	3. Recipient's Catalog No.
NASA TP-2266		

4. Title and Subtitle	5. Report Date
Dynamic Behavior of Spiral-Groove and Rayleigh-Step Self-Acting Face Seals	January 1984
	6. Performing Organization Code: 505-33-52
7. Author(s): Eliseo DiRusso	8. Performing Organization Report No.: E-1754
	10. Work Unit No.
9. Performing Organization Name and Address: National Aeronautics and Space Administration, Lewis Research Center, Cleveland, Ohio 44135	11. Contract or Grant No.
	13. Type of Report and Period Covered: Technical Paper
12. Sponsoring Agency Name and Address: National Aeronautics and Space Administration, Washington, D.C. 20546	14. Sponsoring Agency Code

15. Supplementary Notes

16. Abstract

Tests were performed to determine the dynamic behavior and establish baseline dynamic data for five self-acting face seals employing Rayleigh-step lift-pads and inward pumping as well as outward-pumping spiral grooves for the lift-generating mechanism. The primary parameters measured in the tests were film thickness, seal seat axial motion, and seal frictional torque. The data show the dynamic response of the film thickness to the motion of the seal seat. The inward-pumping spiral-groove seals exhibited a high-amplitude film thickness vibratory mode with a frequency of four times the shaft speed. This mode was not observed in the other seals tested. The tests also revealed that high film thickness vibration amplitude produces considerably higher average film thickness than do low amplitude film thickness vibrations. The seals were tested at a constant face load of 73 N (16.4 lb) with ambient air at room temperature and atmospheric pressure as the fluid medium. The test speed range was from 7000 to 17 000 rpm. Seal tangential speed range was 34.5 to 83.7 m/sec (113 to 274 ft/sec).

17. Key Words (Suggested by Author(s))	18. Distribution Statement
Face seal Self-acting seal Gas bearing Spiral groove seal Rayleigh-step seal	Unclassified - unlimited STAR Category 07

19. Security Classif. (of this report)	20. Security Classif. (of this page)	21. No. of pages	22. Price*
Unclassified	Unclassified	18	A02

*For sale by the National Technical Information Service, Springfield, Virginia 22161

NASA-Langley, 1984